ELECTRONIC SUPPLEMENTARY INFORMATION

Physical mechanisms of the Sec machinery operation

Ekaterina Sobakinskaya,* Frank Müh

Institute for Theoretical Physics, Johannes Kepler University Linz, Altenberger Strasse 69, A-4040 Linz, Austria.
**E-mail: esobakinskaya@gmail.com*

Supplementary figures

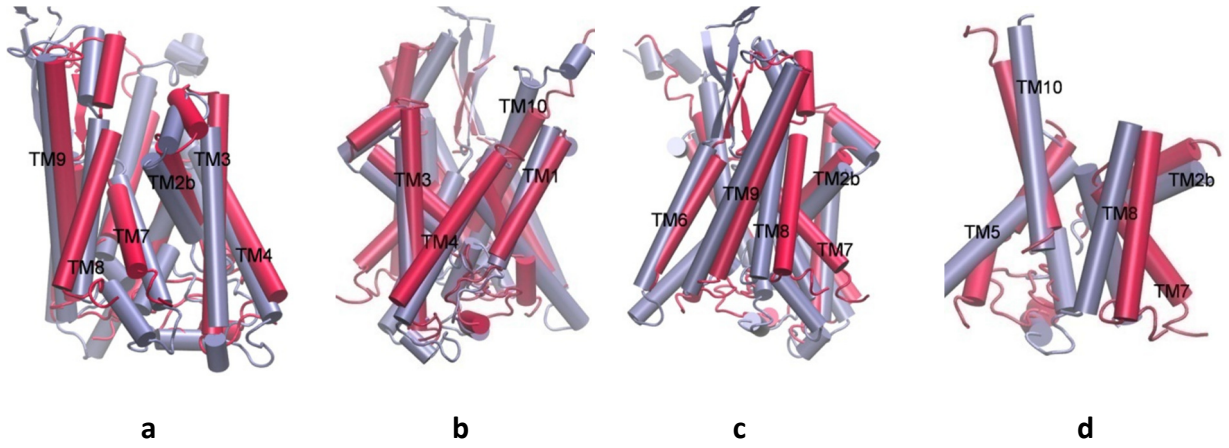

Fig. S1 Overlay of the structures 5AWW (iceblue) and 5EUL (red color). The views in a - d are all along the membrane plane and differ in orientation.

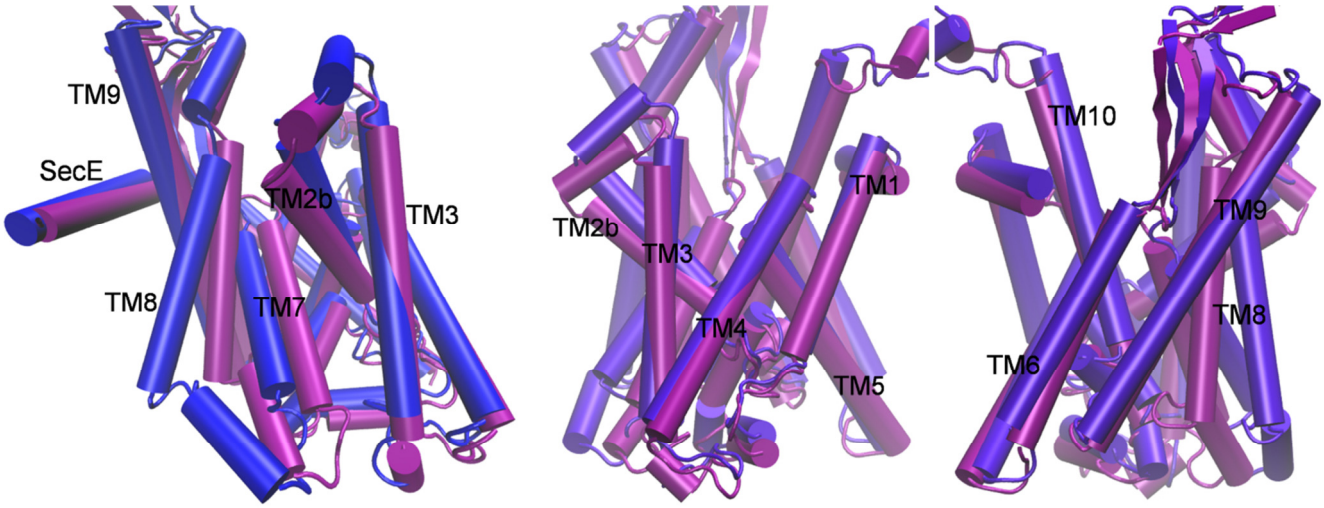

Fig. S2 Overlay of SecYEG in the closed (5AWW, magenta) and half-open (blue) conformations viewed from different angles.

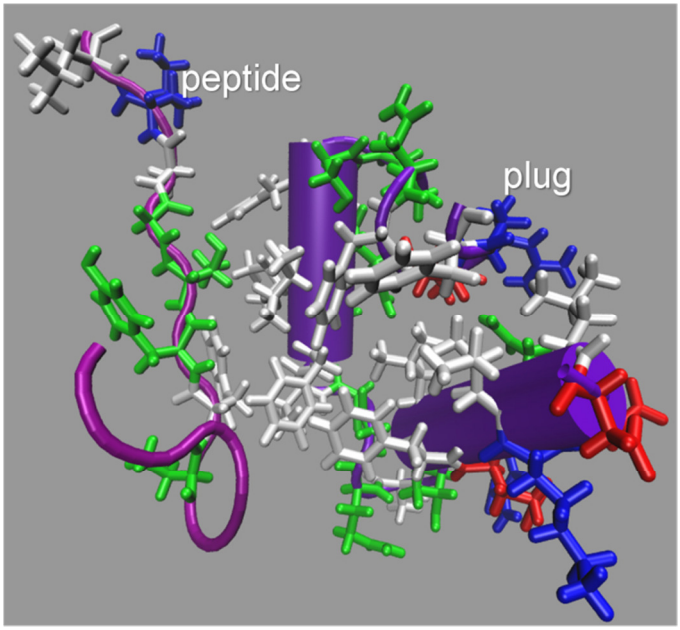

Fig. S3 Interaction between the peptide and the plug in the half-open channel. The snapshot shown of the peptide near the plug corresponds to $z = 0.19$ Å. The backbones of the peptide and the plug are given in cartoon representation and coloured magenta and violet, respectively. The selected amino acid residues are shown explicitly and coloured according to their type: white, hydrophobic; green, polar; blue, positively charged; red, negatively charged.

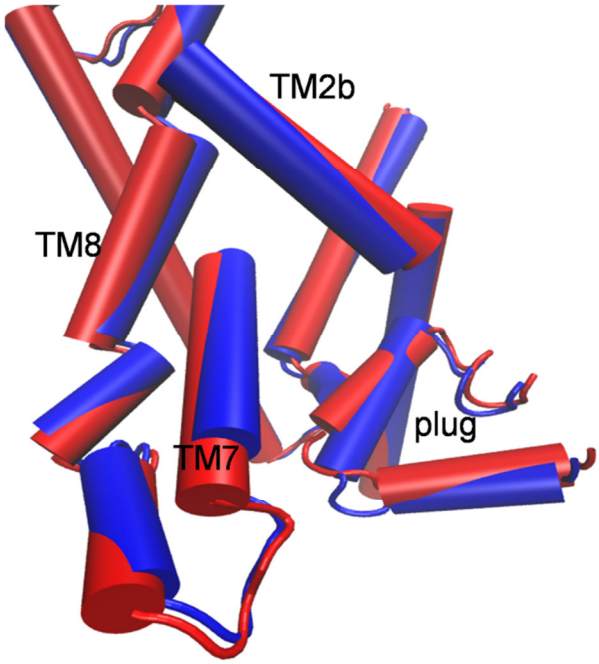

Fig. S4 Overlay of half-open channel conformations corresponding to the first (blue) and the last (red) window of the US simulations.

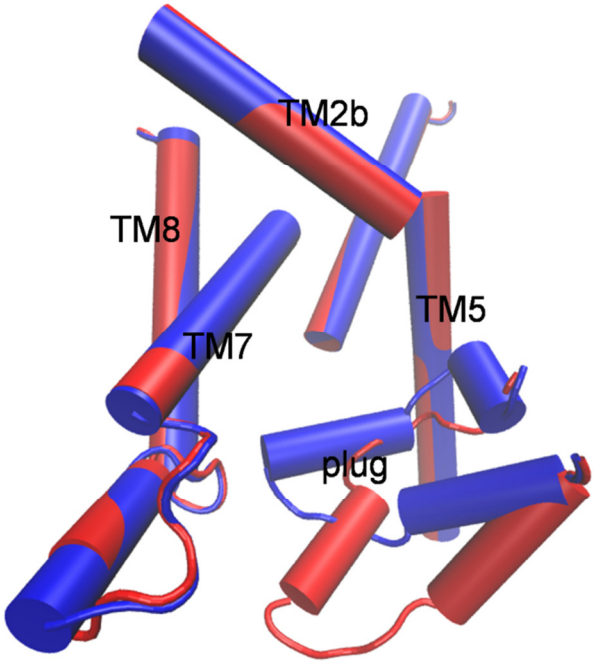

Fig. S5 Overlay of open channel conformations corresponding to the first (blue) and the last (red) window of the US simulations. The plug moves down while the peptide is transported across the channel.

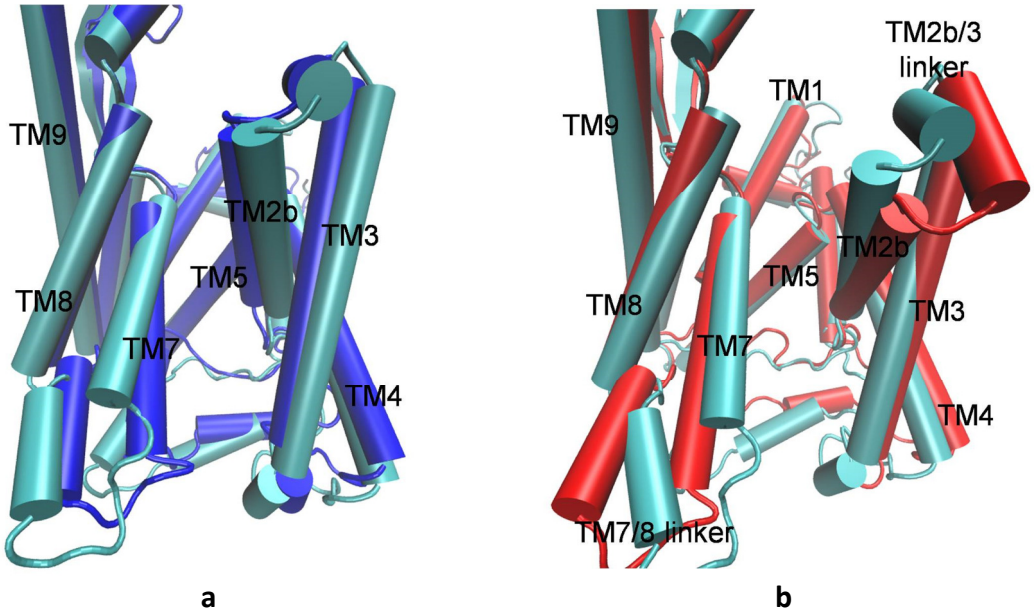

Fig. S6 Changes in the channel´s conformation in the ADP-bound state for simulations without (a) and with (b) applied voltage. Overlay of the starting configuration (cyan) and the last frames of the relax- (blue) and volt-simulation (red).

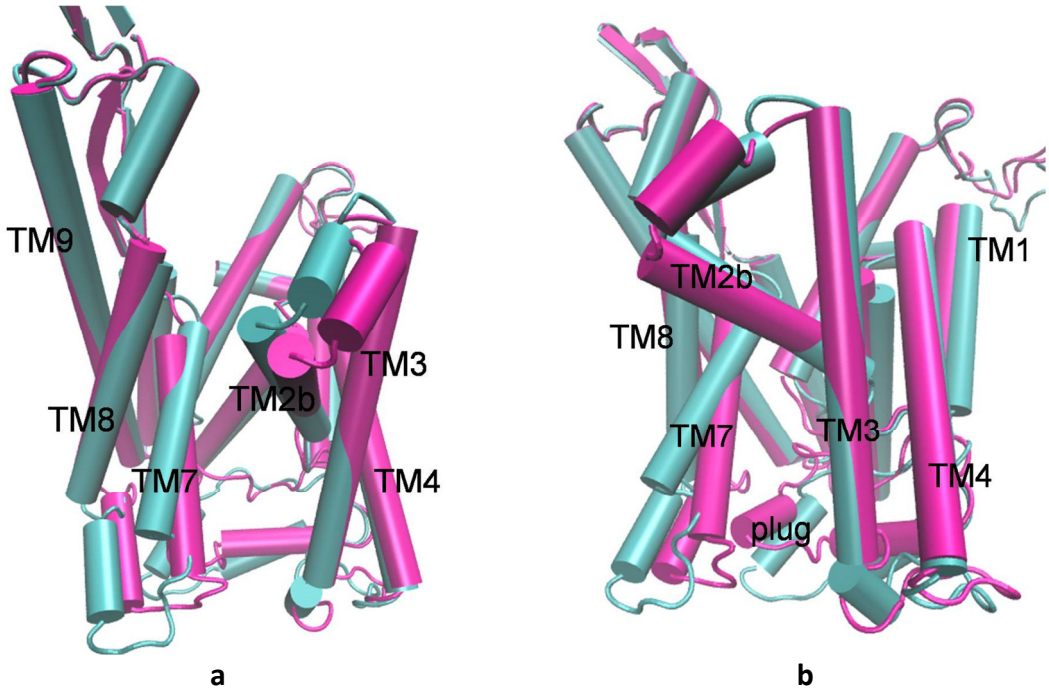

Fig. S7 Changes in the channel´s conformation in the ATP-bound state. Overlay of the starting configuration (cyan) and the last frame of the simulation with applied voltage (magenta). Snapshots are taken along the y (a) and x axis (b).

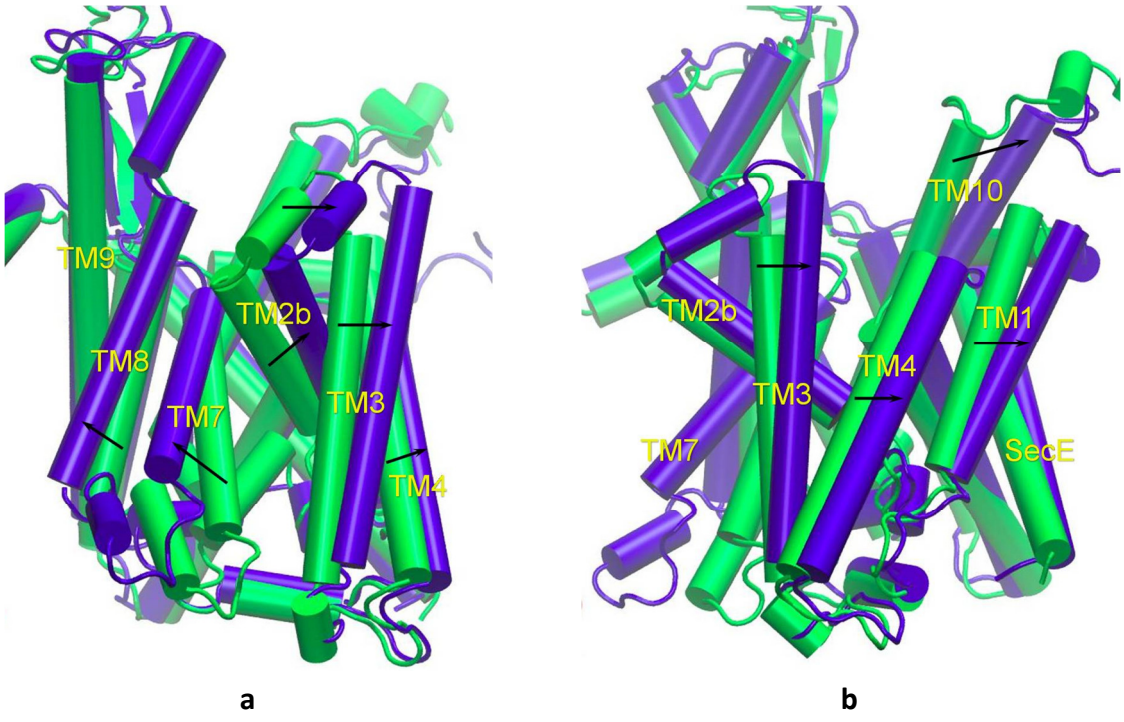

Fig. S8 Overlay of the closed (5AWW, green) and open (blue) conformations of SecYEG: (a) and (b) correspond to side views along the y and x axes, respectively. The small black arrows indicate the motion of the corresponding helices upon opening of the translocon.

Details of structural analysis

A1. Lethal mutations

Among the most extreme mutations, which cause lethality, combined with L108R (*prlG1*) in SecE, are adjacent residues I408N, L407R, in TM10 and I278N in TM7. Interestingly, none of the residues of TM7 and TM10 is in direct contact with residue Leu 108 of SecE. At the same time, the above residues are involved in interactions with TM5 (in *E. coli*): Ile 278 (TM7) ↔ Ile 191, Phe 192 (TM5); Ile 408 (TM10) ↔ Ile 195 (TM5); Leu 108 (SecE) ↔ Ala 197, Val 196 (TM5). The above substitutions introduce polar or charged amino acids, thus, disrupting the hydrophobic contacts. The residue Leu 407, instead, points toward TM9. The lethality caused by this mutation, when combined with *prlG1*, can be explained by a shift of TM10 towards TM9 due to an increased interaction between Leu 407 and Thr 382, thus, weakening contacts between TM10 and TM5. In contrast, the mutant, which carries both L407R (TM10) and A277E (TM7) substitutions, shows no lethality with *prlG1*. In this case, we suggest that interaction between TM7 and TM10 stabilizes the latter, preventing it from shifting. From these results, we deduce an involvement of TM5 in the translocation process.

A2. Results from K.Sato et al. (1997) J. Biol. Chem. 272, 5880 - 5886

The authors studied the stepwise translocation of short hydrophobic segments in ProOmpA across membrane vesicles of *E. coli* in the absence of a proton motive force. The segments H1 and H2 were composed of SerValValValLeu and ValAspTyrLeuIle, respectively. It was demonstrated, that when the concentration of ATP was low, H2 was proven to be a stronger arrest signal compared to H1, which can be explained by the presence of Tyr in the former. When the protein includes both segments, the replacement of H1 with a sequence containing Trp leads to a strong arrest of the transport. Interestingly, the substitution of H1 and H2 with hydrophilic sequences that still contain Trp did not result in a continuous translocation. Therefore, it is not the hydrophobic nature of the protein segments *per se*, but the bulkiness of residues that increases the barrier for translocation.

Method details

M1. Application of external forces

External forces – provided by different protocols of NAMD – were applied to (i) pull the helices and (ii) monitor translocation of the peptide through the channel.

(i) To create the transit-half configuration, the lateral gate of the structure 5AWW was opened by constant-force pulling of helices TM2, TM7, and TM8, employing a TCL protocol of NAMD [M1-1]. The force was applied to all atoms of a pulled residue, while other helices were kept fixed. The total time of TM2 shifting was 550 ps. The shifts of TM8 and TM7 to new positions was produced by a 1 ns simulation each. The applied forces were recalculated every 500 steps. The simulations were carried out under the conditions described in the *General information* Section.

In the case of the open channel, the helices TM8, TM7, TM2b, TM5, TM9, and TM10 were pulled to the corresponding positions in the 5EUL structure, thus, obtaining transit-open. The total time of shifting for each helix varied between 550 and 960 ps. The same TCL protocol and procedure as for the transit-half configuration were applied in this case.

(ii) SMD with constant velocity protocol, implemented in NAMD, was used to pull a peptide through SecYEG along the z axis to create windows for umbrella sampling (US). The simulations were performed with a step of 1 fs. (Other conditions are described in the *General information* Section.)

For the half-open channel, the SMD trajectory of 33 ns was performed with a velocity of 1 Å/ns and a force constant of 36 kcal/(mol Å^2). To prevent drift of the translocon, harmonic constraints energy function with exponent were applied along the z axis for the protein backbone of SecY, except the plug and TM9/TM10 linker.

In the case of the open channel, the same harmonic constraints were applied along all axes, keeping the channel in the open state and mimicking strong interaction with SecA. The total simulation time was 30 ns.

[M1-1] https://www.ks.uiuc.edu/Training/Tutorials/.

M2. Simulation of the plug movement

A difficulty in studying the conformational transition from the closed to the open state arises from the simultaneous movement of many helices involving a huge number of coordinates. To obtain a free-energy profile, we had to significantly reduce the problem and concentrate on the conformational transition of the plug only. To determine the position of the plug and understand its pathway from the closed to the open state, we applied the following procedure.

As a first step, we shifted the key-set helices to the positions prescribed by the 5EUL structure, keeping the plug fixed in the closed conformation. This procedure resulted in the system being in a transition state between the closed and open configurations. Under these conditions, the further dynamics of the plug is guided by multiple interactions with TM helices. To mimic the conformational transitions in the native opening, we stimulated motion of the plug driven by the same forces. Taking into account the above considerations about coupling between the plug and other TM helices, we assumed that the major contribution originates from the interactions with TM5, TM2b and the TM9/10 linker. Hence, to determine a transition pathway, we computed a free-energy landscape as a function of pairwise distances between the plug and these helices (defined in M3), keeping the TM helices fixed in the open positions. The schematic comparison of the plug´s trajectory (in the coordinate space) during our simulations and in the process of native opening is shown in Fig. 5d.

We projected the high-dimensional space of variables responsible for motion of the key-set helices and the plug on a 2D map of representative coordinates r_h and r_p. In the course of the native opening, the cooperative movement of the SecYEG helices plays an important role that is represented by the synchronous changing of the representative coordinates along the green curve in Fig. 5d. (We assume here that the conformational transformation leads to an increase of the coordinate´s magnitude.) In our simulation, we started from a configuration, where the helices were locked in the open positions, having a coordinate r_h(open), while the plug was still in the closed state r_p(closed). A biasing potential was applied to make the plug explore the potential surface, determined by the interactions above. Thus in our modeling, transition of the plug to the open configuration goes along the blue and red trajectories in Fig. 5d. Here we underline, that the free-energy landscape, explored in our simulations, depends on distances between the plug and corresponding helices. Thus, provided all relevant distances are explored and convergence is reached, we expect the simulated free-energy profiles to be realistic.

M3. Metadynamics

Well-tempered metadynamics with a temperature bias of 2700 K was performed to sample the free-energy landscape of the plug position. The collective variables, d_1, d_2, d_3, included three center-of-mass (COM) distances between residues of the plug and helices TM2b, TM5 and the TM9/10 linker. The first distance, d_1, was measured between the plug residues 62 to 64 and residues 76 to 78 of TM2b. The second reaction coordinate, d_2, sampled the distance between residues 54 to 61 of the plug and residues 188 to 191 of TM5. The third variable, d_3, included the same plug residues as the second one and linker residues 392 to 394. The hill weight and width were taken to be 0.2 and 1.0, respectively. The new hill was added to the metadynamics potential after 500 steps. Soft harmonic constraints with the force constant 0.5 kcal/(mol·Å^2) were applied for lipids around the channel, the backbone of the key-set helices and SecE. To prevent the ion flux, we also constrained chloride and potassium ions with 0.1 kcal/(mol·Å^2). Other conditions of the simulations are described in the *General information* Section.

To monitor the convergence of the potential, we produced trajectories with different simulation times ranging from 2 ns to 60 ns. For every trajectory, we determined a transition path (from closed to open conformation), going through neighboring minima in the free-energy surface (Fig. S9). Obviously, the flexibility of the linker TM9/10 and the plug leads to a variation in the minima positions. Therefore, the criterion for a sufficient simulation time was the convergence of a generalized distance between transition paths *s* and *r* defined as:

$$g^{(r,s)} = \sum_{i}^{N} \sqrt{\left(1 - \frac{r_i^{(1)}}{s_i^{(1)}}\right)^2 + \left(1 - \frac{r_i^{(2)}}{s_i^{(2)}}\right)^2 + \left(1 - \frac{r_i^{(3)}}{s_i^{(3)}}\right)^2 + \left(1 - \frac{e_i^{(r)}}{e_i^{(s)}}\right)^2}$$

where $r_i^{(k)}$and $s_i^{(k)}$ are collective variable k of the transition paths s and r in minima i, $e_i^{(r)}$and $e_i^{(s)}$are free-energy values at the corresponding minima, and N is the total number of minima (Table S1). The final conformation of the plug was obtained from the 40 ns-trajectory. Here, we selected the minima from the free-energy landscape, which corresponds to a plug position close to the one of the 5EUL structure (Fig. S10 and S11).

Table S1. Generalized distance $g^{(r,s)}$ between transition pathways obtained from metadynamics trajectories of different simulation time.

$r \leftrightarrow s$	5 ns ↔ 10 ns	10 ns ↔ 20 ns	20 ns ↔ 40 ns	40 ns ↔ 60 ns
$g^{(r,s)}$	16.02	12.60	11.35	11.27

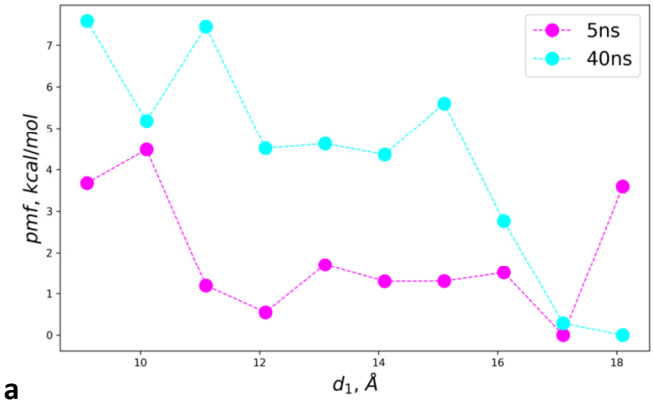

a

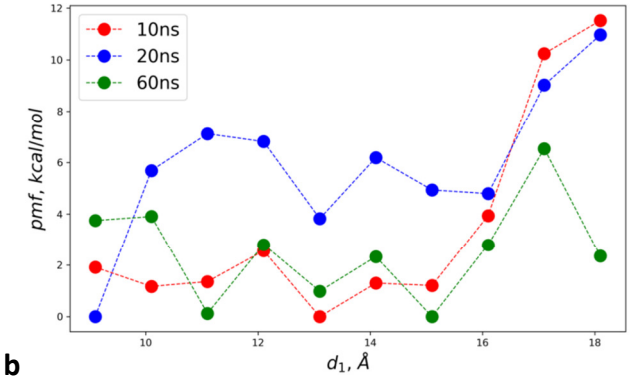

b

Fig. S9 Transition pathways for different metadynamics simulations with simulation times of (a) 5 and 40 ns as well as (b) 10, 20, and 60 ns.

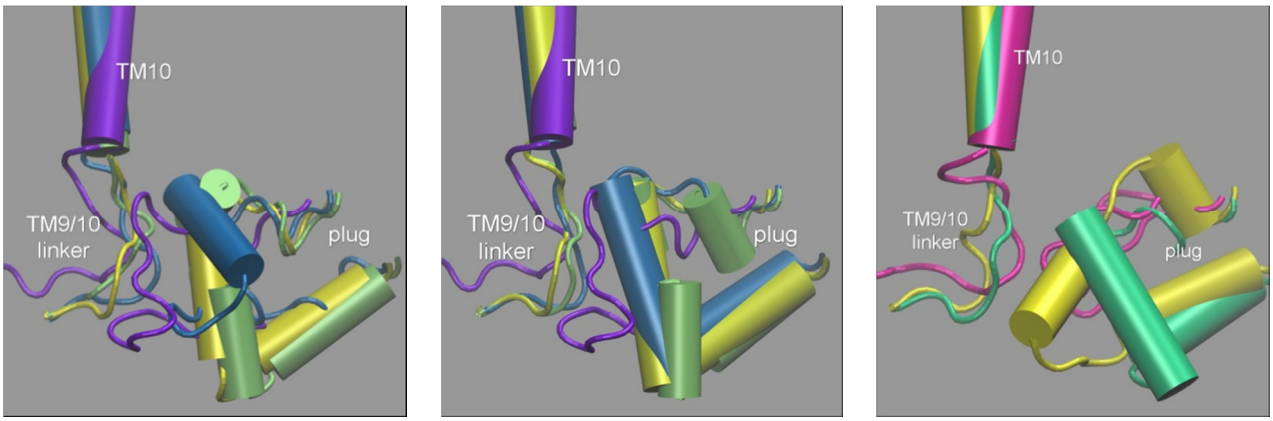

a **b** **c**

Fig. S10 Configuration of the plug in the PMF minima (Fig. S9) for metadynamics trajectories of different simulation times. The minima are distinguished by the first collective variable d_1: (a) d_1 = 13 Å, green, yellow and blue correspond, respectively, to trajectories of 10, 20 and 60 ns; (b) d_1 = 15 A, colours like in (a); (c) d_1 = 17 Å, yellow and green correspond, respectively, to 5 and 40 ns trajectories. The obtained conformations are overlaid with the open channel structures 6ITC (violet) and 5EUL (magenta).

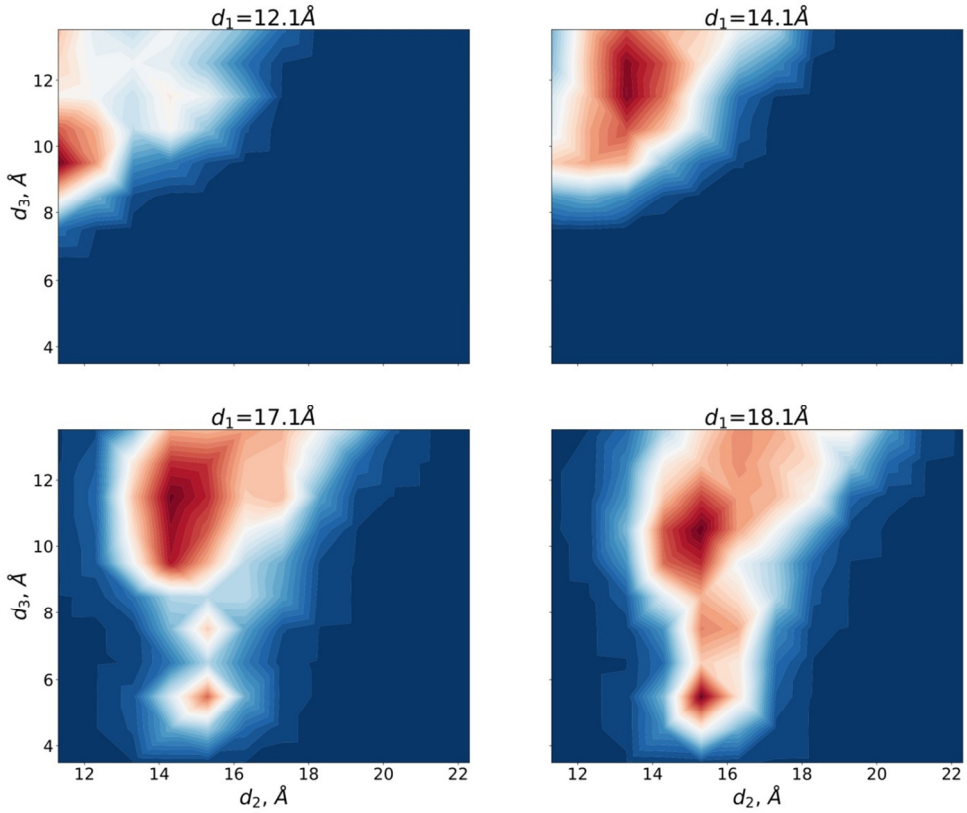

Fig. S11 Free-energy profiles for selected minima of the metadynamics from the 40 ns trajectory.

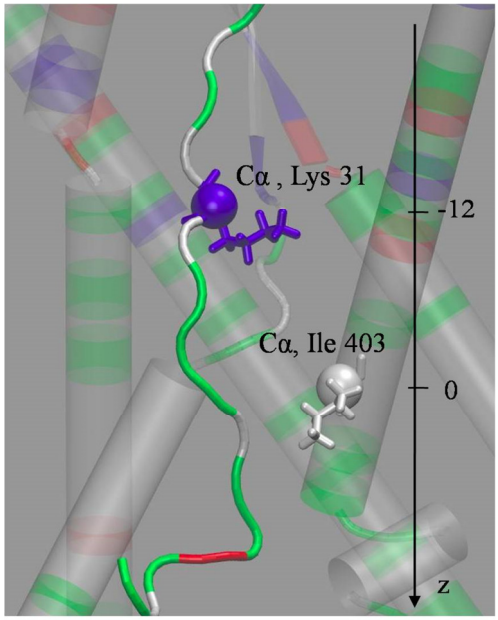

Fig. S12 Definition of a reaction coordinate for the umbrella sampling simulations: distance between the C_α atom of Lys 31 (blue) of the peptide and the C_α atom of Ile 403 (white) in the PR. The z coordinate of the C_α-atom of Ile 403 (white sphere) defines the origin of the z axis (in Å). The C_α-atom of Lys 31 (blue sphere) shown is close to the position $z = -12$ Å.

M4. Umbrella sampling

The reaction coordinate for US [M4-1, M4-2, M4-3] was chosen as the distance between the C_α atom of Lys 31 of the peptide and the C_α atom of Ile 403 in the PR (Fig. S12). The span of the reaction coordinate was subdivided into windows with ≤ 1 Å spacing (Fig. S13). For each window, we run an independent simulation of 12 ns (with a time step of 1 fs). The force constants were selected to be in the range between 2.5 and 9 kcal/(mol Å^2), which allows efficient sampling for every reaction coordinate and overlap of neighboring windows. In the case of the open channel, we put soft harmonic restraints with force constant 0.4 kcal/(mol Å^2) for the key-set helices and the plug for every window, thus, imitating binding with the translocation partner.

We applied the Weighted Histogram Analysis Method (WHAM) [M4-3, M4-4] to construct the PMF from the sorted trajectory files obtained with US. The unbiased probability distribution of a system along the reaction coordinate is calculated by a weighted average of the distributions of the individual windows. The weights for the windows are chosen in order to minimize the statistical error of the whole distribution. Version 2.0.9 of the WHAM package was used [M4-5]. The first 1 ns in each window was treated as an equilibration phase and, hence, ignored for post-processing.

[M4-1] G. M. Torrie and J. P. Valleau (1974) *Chem. Phys. Lett.* 28, 578 - 581.

[M4-2] G. M. Torrie and J. P. Valleau (1977) *J. Comput. Phys.* 23, 187 - 199.

[M4-3] J. Kästner (2011) *WIREs Comput. Mol. Sci.* 1, 932 - 942.

[M4-4] S. Kumar, D. Bouzida, R. H. Swendsen, P. A. Kollman and J. M. Rosenberg (1992) *J. Comput. Chem.* 13, 1011 - 1021.

[M4-5] http://membrane.urmc.rochester.edu/?page_id=126.

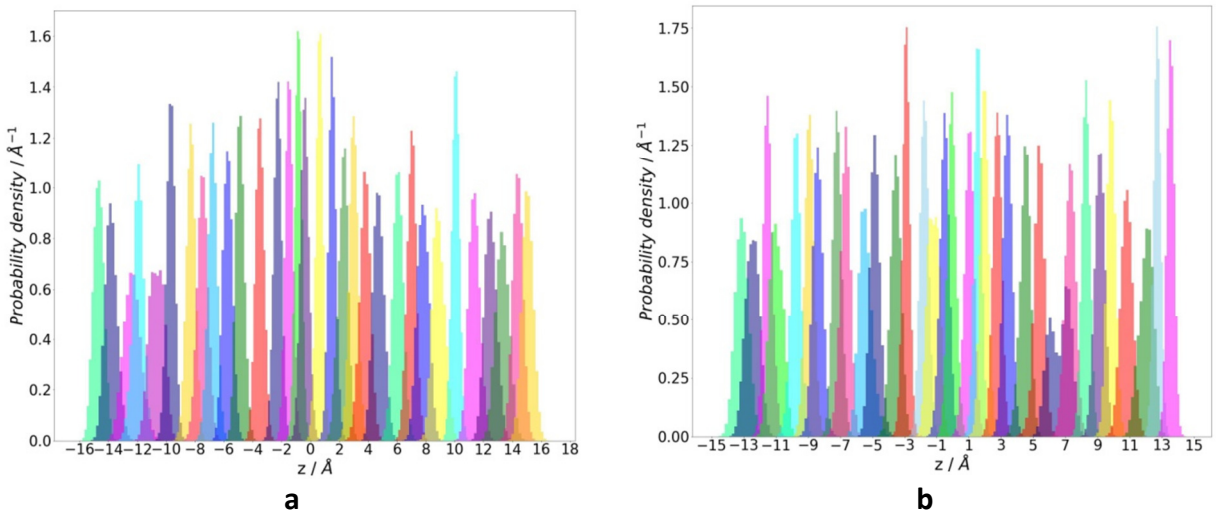

Fig. S13 US windows generated for the calculation of the PMF profile for the translocation of the peptide inside (a) half-open and (b) open SecYEG.

M5. Interaction of the plug with solvent

To reveal how solvent-induced forces exerted on the plug affect the conformational transition between the open and closed states, we calculated interaction energies between plug and water for the half-open and the open structure (without the peptide inside). The structures imitate the initial phase of translocation, when we can neglect the coupling between the translocated peptide and the plug. A harmonic restraint potential with a force constant of 0.3 and 0.03 kcal/(mol·Å^2) was imposed on the protein backbone and ions. The NAMD protocol for pairwise interactions was employed to compute electrostatic and van der Waals energies for every frame [M5-1]. The data set obtained from each trajectory included 60 points and represented the interaction energy averaged over 500 ps. The computed difference between energies in open and half-open conformations was analyzed with the independent-samples t-test (Student´s t-test) performed with the SPSS Statistics package (for details, see [M5-2]). The test demonstrated statistically significant differences between the means of the interaction energies.

[M5-1] E. Sobakinskaya, H. Krobath, T. Renger, F. Müh (2021) *Phys. Chem. Chem. Phys.* 23, 25830 - 25840.
[M5-2] https://statistics.laerd.com.

M6. Application of external electric field

As part of the research aiming at understanding the influence of $\Delta\Psi\mathrm{H}^+$ on protein translocation, we explored the effect of the membrane potential on the channel´s conformation in the ATP- and ADP-bound state of the Sec machinery. For this purpose, we selected an open conformation with the peptide inside, which corresponds to the US window with $z = 14$ Å. This frame was used as a starting conformation for a 400 ns simulation, where external voltage was applied along the z axis with a polarity corresponding to a positive sign inside the periplasm. (Before the actual dynamics, we performed an equilibration of 20 ns.) To observe an effect along a relatively short trajectory, an external field equivalent to 1.1 V was used during the first 200 ns. For the second half of the trajectory, the voltage was reduced to 0.3 V, which was enough to keep the channel in the open state ("volt-trajectory"). In the case of the ADP-bound state, to better understand conformational alterations, we run also a 400 ns trajectory starting from the same conformation, but without external voltage ("relax-trajectory").

To mimic the strong interaction between translocon and SecA in the ATP-bound state, we imposed soft restraints on the channel with a force constant of 0.3 kcal/(mol Å^2) as shown in

Fig. S14. All other details of the simulations are provided in *General Information*. In the case of the ADP-bound conformation, restraints with the same force constant were applied to the backbone of TM9, imitating weak binding with SecA and preventing drifting of the channel. All other details of the simulations are provided in *General Information*.

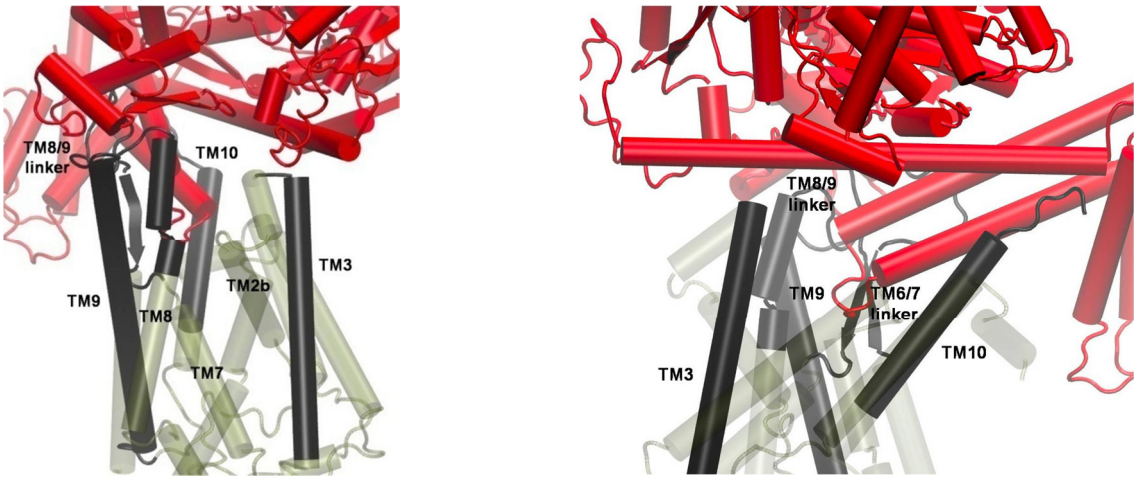

Fig. S14 Interaction between SecA (red) and selected helices and linkers of the translocon (black) based on the 6ITC and 5EUL structures. Other helices are shown in tan color and transparent representation. The constraints were imposed on the residues colored by black.

Analysis of the simulations involved the comparison of the dynamics of selected helices for trajectories with and without external field (Fig. S15, S16). For helices TM10, TM2b, TM5 and the plug, we computed the difference between the center of mass (COM) of selected residues, Δr_i, of the initial state with coordinates (x_0, y_0, z_0), and the position along the trajectory (x_i, y_i, z_i): $\Delta r_i = \sqrt{(x_0 - x_i)^2 + (y_0 - y_i)^2 + (z_0 - z_i)^2}$, where i is the number of the trajectory frame. Moreover, to further characterize the influence of the voltage, changes in distances TM7-TM10 and TM7-plug, Δd_i, with respect to the starting conformation were monitored for every simulation: $\Delta d_i = d_0 - d_i$, where d_0 and d_i are the distances for the initial state and trajectory frame i, respectively. The results of the dynamics simulations displayed significant variations of the polar angle φ of TM7 and distances between the PR residues. The former were analyzed similarly to distances: $\Delta\varphi_i = \varphi_0 - \varphi_i$, where φ_0 and φ_i are a polar angles for the initial state and trajectory frame i, respectively. The PR distances, *d*, TM5-TM7 and TM2b-TM10, are calculated between the COM of Ile 188 and Ile 275 as well as Ile 81 and Ile 403, respectively. To get rid of the thermal fluctuations and reveal the trend, we applied the spline function for the calculated parameters.

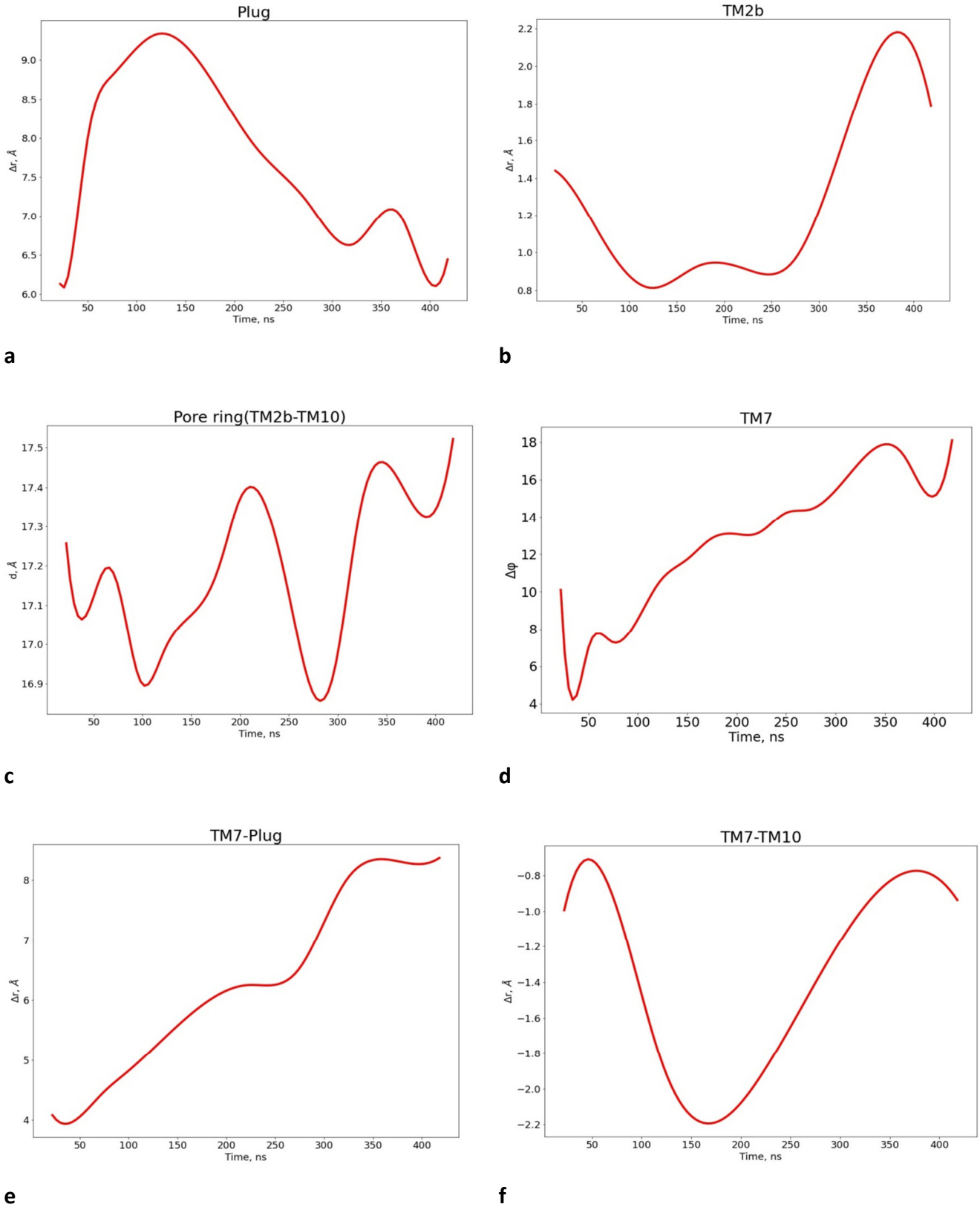

Fig. S15 Dynamics of the channel´s collective variables in the ATP-bound state: (a, b) shift in COM position of the plug and TM2b, respectively; (c) distance between the COM of the PR residues Ile 81 (helix TM2b) and Ile 403 (TM10); (d) change of the polar angle of TM7 with respect to initial value; (e, f) changes in the distances between TM7 and the plug as well as between TM7 and TM10, respectively.

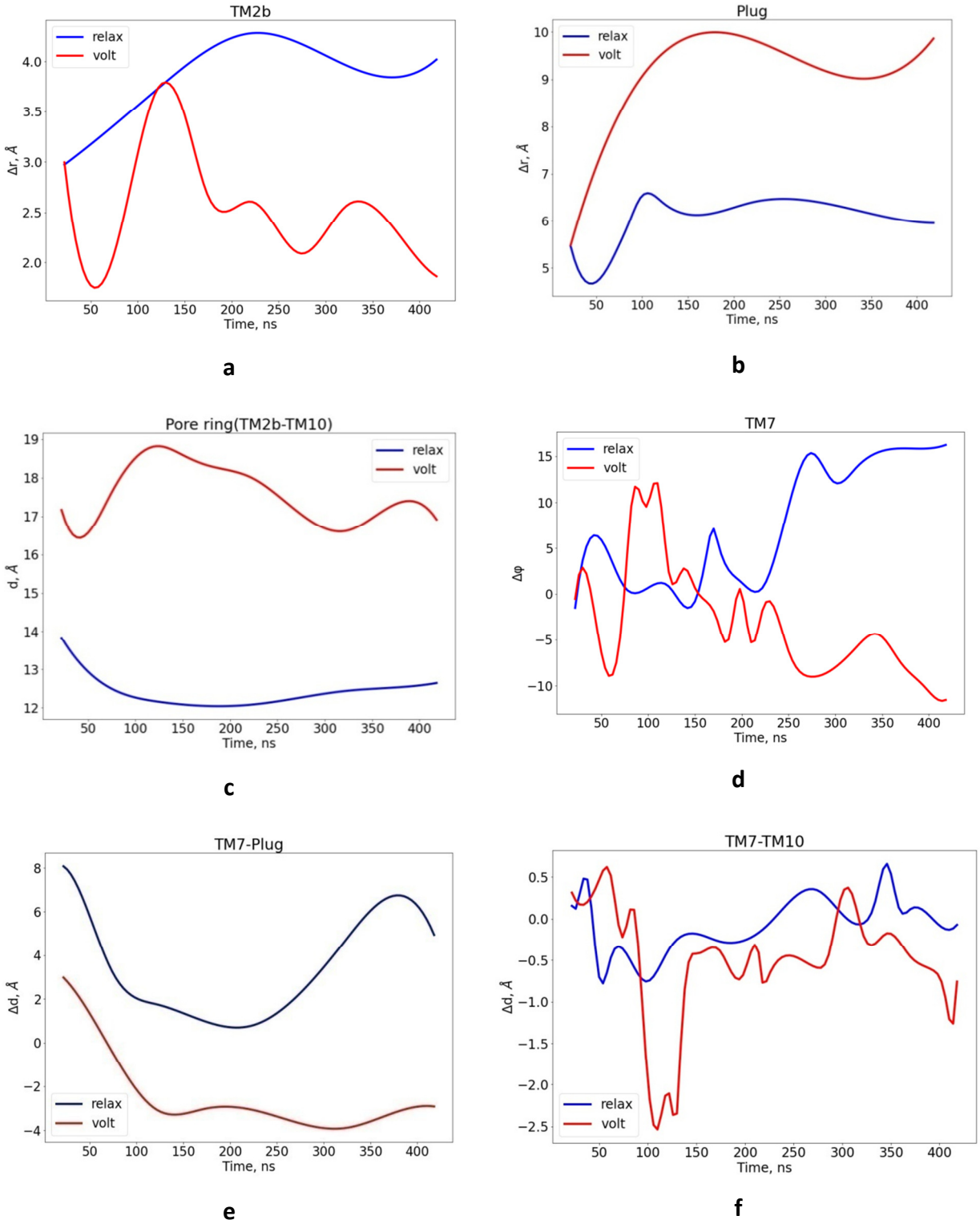

Fig. S16 Dynamics of the channel´s collective variables in the ADP-bound state: (a, b) shift in COM positions of TM2b and the plug, respectively; (c) distance between the COM of the PR residues Ile 81 (helix TM2b) and Ile 403 (TM10); (d) change of the polar angle of TM7 with respect to initial value; (e, f) changes in the distances between TM7 and the plug as well as between TM7 and TM10, respectively. The curves, corresponding to the volt- and relax-trajectories are coloured red and blue, respectively.

For both ATP- and ADP-bound conformations, we calculated the ion flux, counting all ions that crossed the position of the z coordinate of the pore ring COM and moved at least 10 Å beyond it. The total number of ions crossing the PR during the volt-simulations is shown in Fig. S17. The PR COM was defined with respect to the four Ile residues forming the PR.

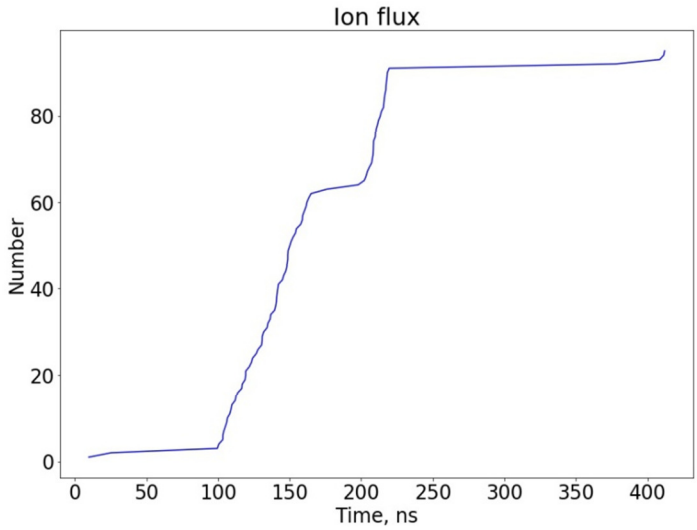

Fig. S17 Total number of ions crossing the pore ring in the volt-simulation for the ADP-bound state.

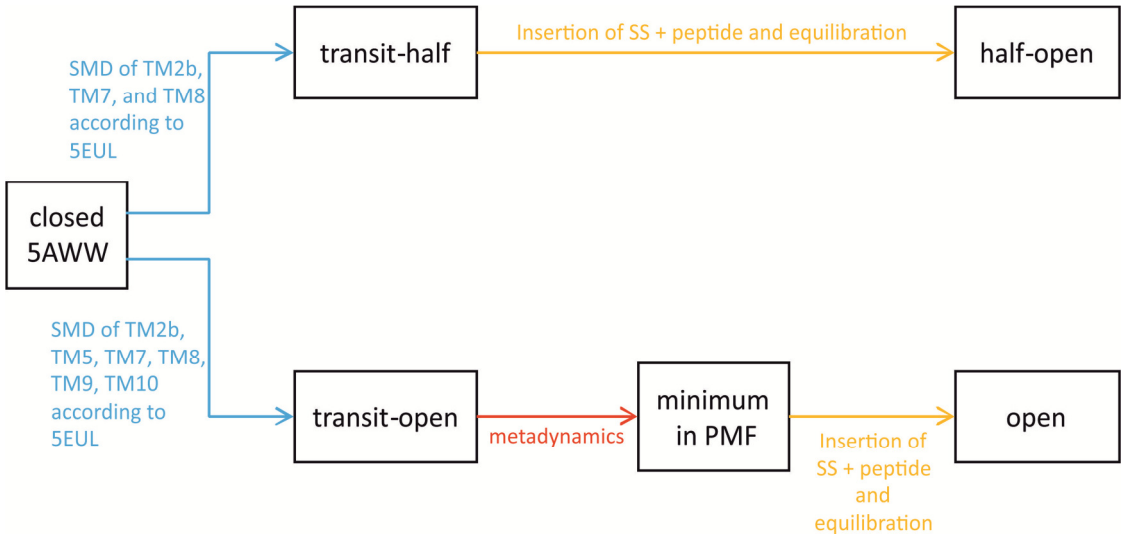

Fig. S18 Flow chart illustrating the preparation of the various SecYEG simulations starting from the closed channel (PDB ID 5AWW) and taking into account structural information from the open channel according to PDB ID 5EUL.

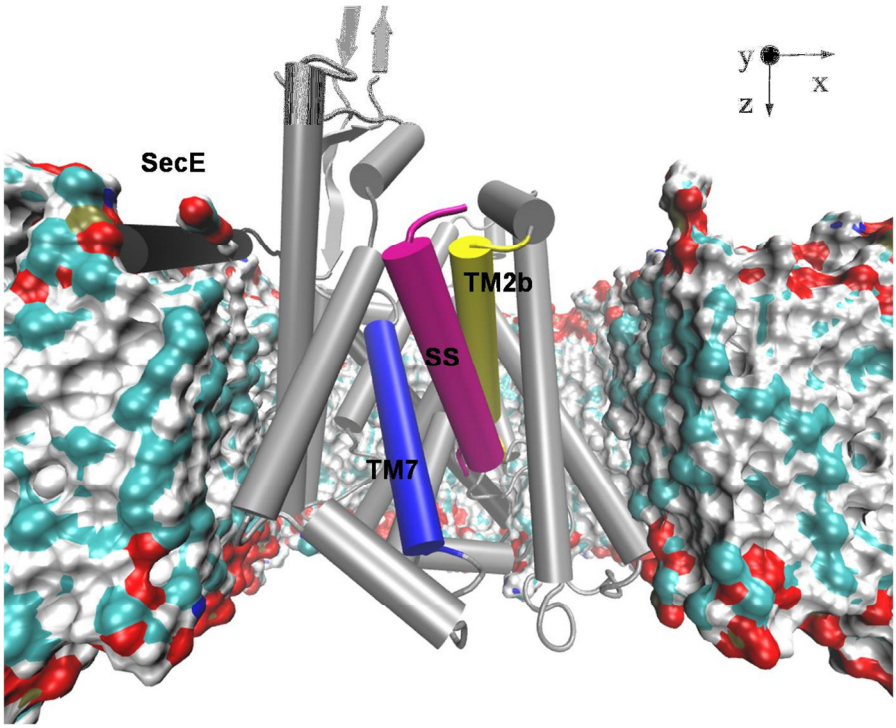

Fig. S19 SecYEG in the conformation "half-open" (cartoon representation) embedded in the membrane. The signal sequence (SS, magenta) is inserted into the lateral gate between TM7 (blue) and TM2b (yellow).

Table S2. Names, origins, and descriptions of the various SecYEG structures investigated in the present work and shown in the flowchart in Fig. S18.

Name of structure	Origin	Description
5AWW	PDB	Crystal structure of the closed SecYEG. For further simulations, the structure was embedded into a lipid bilayer and water box with KCl.
transit-half	obtained from 5AWW	SMD was used to pull helices TM2b, TM7 and TM8 on the positions of those in the 5EUL structure.
half-open	obtained from transit-half	The signal sequence with peptide was inserted, followed by minimization and equilibration.
transit-open	obtained from 5AWW	SMD was used to pull helices TM2b, TM5, TM7, TM8, TM9 and TM10 on the positions of those in the 5EUL structure.
open	obtained from transit-open	Metadynamics was used to determine the position of the plug in the open conformation. Then the signal sequence with peptide was placed inside, followed by minimization and equilibration.